PLOS ONE

RESEARCH ARTICLE

Cooling induces phase separation in membranes derived from isolated CNS myelin

Julio M. Pusterla[1], Emanuel Schneck[2], Sérgio S. Funari[3], Bruno Démé[4], Motomu Tanaka[5,6], Rafael G. Oliveira[1]*

1 Centro de Investigaciones en Química Biológica de Córdoba (CIQUIBIC)-Departamento de Química Biológica, Facultad de Ciencias Químicas, Universidad Nacional de Córdoba, Ciudad Universitaria, Córdoba, Argentina, **2** Biomaterials Department, Max Planck Institute of Colloids and Interfaces, Potsdam, Germany, **3** HASYLAB at DESY, Hamburg, Germany, **4** Institut Laue-Langevin (ILL), Grenoble, France, **5** Biophysical Chemistry II, Institute of Physical Chemistry and BIOQUANT, University of Heidelberg, Heidelberg, Germany, **6** Institute for Integrated Cell-Material Sciences (WPI iCeMS), Kyoto University, Kyoto, Japan

* rafaeltum@gmail.com

Citation: Pusterla JM, Schneck E, Funari SS, Démé B, Tanaka M, Oliveira RG (2017) Cooling induces phase separation in membranes derived from isolated CNS myelin. PLoS ONE 12(9): e0184881. https://doi.org/10.1371/journal.pone.0184881

Editor: Patrick van der Wel, University of Pittsburgh School of Medicine, UNITED STATES

Received: May 19, 2017

Accepted: September 3, 2017

Published: September 15, 2017

Data Availability Statement: All relevant data are within the paper and its Supporting Information files.

Funding: This work was supported by Consejo Nacional de Investigaciones Científicas y Técnicas (CONICET) grant no. 11220150100621CO, Fondo para la Investigación Científica y Tecnológica (FONCyT) grant no. 2012-2583, Ministerio de Ciencia, Tecnología e Innovación Productiva (Argentina) and Secretaría de Ciencia y Tecnología, University of Córdoba (SECyT-UNC) to RGO. RGO is career investigators of CONICET (Argentina).

Abstract

Purified myelin membranes (PMMs) are the starting material for biochemical analyses such as the isolation of detergent-insoluble glycosphingolipid-rich domains (DIGs), which are believed to be representatives of functional lipid rafts. The normal DIGs isolation protocol involves the extraction of lipids under moderate cooling. Here, we thus address the influence of cooling on the structure of PMMs and its sub-fractions. Thermodynamic and structural aspects of periodic, multilamellar PMMs are examined between 4˚C and 45˚C and in various biologically relevant aqueous solutions. The phase behavior is investigated by small-angle X-ray scattering (SAXS) and differential scanning calorimetry (DSC). Complementary neutron diffraction (ND) experiments with solid-supported myelin multilayers confirm that the phase behavior is unaffected by planar confinement. SAXS and ND consistently show that multilamellar PMMs in pure water become heterogeneous when cooled by more than 10–15˚C below physiological temperature, as during the DIGs isolation procedure. The heterogeneous state of PMMs is stabilized in physiological solution, where phase coexistence persists up to near the physiological temperature. This result supports the general view that membranes under physiological conditions are close to critical points for phase separation. In presence of elevated Ca^{2+} concentrations (> 10 mM), phase coexistence is found even far above physiological temperatures. The relative fractions of the two phases, and thus presumably also their compositions, are found to vary with temperature. Depending on the conditions, an "expanded" phase with larger lamellar period or a "compacted" phase with smaller lamellar period coexists with the native phase. Both expanded and compacted periods are also observed in DIGs under the respective conditions. The observed subtle temperature-dependence of the phase behavior of PMMs suggests that the composition of DIGs is sensitive to the details of the isolation protocol.

JMP is doctoral fellow from CONICET. RGO thanks the Alexander von Humboldt Foundation for a postdoctoral research fellowship. The funders had no role in study design, data collection and analysis, decision to publish, or preparation of the manuscript.

Competing interests: The authors have declared that no competing interests exist.

Introduction

Myelin is the membrane system wrapped around neuronal axons that provides neurons with fast signal transmission. Several neurological disorders like Multiple Sclerosis or leukodystrophies are caused by dysfunctional myelin. It is commonly assumed that myelin membranes under physiological conditions contain functional lipid rafts in the form of transiently phase-separated ordered membrane domains [1]. In general, such lipid rafts in membranes emerge at the border of phase coexistence [2–4], and micrographs of monolayers of whole myelin and its purified lipid fraction exhibit stripes and irregular fluctuating shapes, resembling fluctuations near the critical point [5, 6]. For most biochemical-topological studies, for instance on enzyme activity, membrane protein topology, etc., purified myelin membranes (PMMs) are used. PMMs are also the starting material for the isolation of detergent-resistant membrane (DRMs) fractions or detergent-insoluble glycosphingolipid (DIGs) fractions, which are commonly believed to resemble physiological lipid rafts [7–9]. The normal protocols for DIGs isolation involve a step of moderate cooling down to 4˚C.

The structure of myelin has been investigated intensively, mainly with X-rays and neutrons [10, 11]. Most of the work has been performed at room temperature or at very low temperatures (below water freezing) to confirm membrane structure preservation in presence of cryoprotectants [12] as well under electron microscopy sample preparation protocols [13]. However, the behavior of myelin under conditions of moderate cooling (4–15˚C) has remained vastly unexplored [14, 15], despite its great relevance for DIGs and DRMs isolation, at those temperatures. A few studies on nerve myelin dealt with the effect of heating [16, 17]. In a study on the effect of cooling, wide-angle X-ray scattering (WAXS) measurements revealed that myelin lipid acyl chains remain in a disordered state down to low temperatures, as long as the hydration water is still liquid (above -10˚C), and chain crystalline ordering is only observed under conditions of frozen hydration water [18]. No phase coexistence was inferred from those measurements, except for the WAXS work of Chia et al. [19] which suggested a gel-fluid coexistence but could not be reproduced by any other group [18]. To our knowledge there are only two studies about the effect of moderately cooling (up to 4˚C) on intact myelin from homeothermic animals [14, 15] and they were both performed with nerve myelin. Regarding PMMs, which are the starting material for DIGs and DRMs isolation, there is much less work [20–22] and studies on the effect of moderate cooling are entirely lacking.

The objective of this work is thus to determine the thermal behavior of PMMs in a wide temperature range covering both physiological and lipid raft isolation temperatures. Small-angle X-ray scattering (SAXS) and neutron diffraction (ND) are used to identify different membrane phases from their characteristic lamellar periods [23–25] assumed in various biologically relevant aqueous solutions that differently stabilize membrane domains [26, 27]. Certain conditions of cooling or of elevated Ca^{2+} levels are found to promote phase separation. The structural results are complemented with differential scanning calorimetry (DSC) measurements, which reveal the thermodynamics of membrane phase transitions. Finally, isolated DIGs are shown to mimic the non-native phase spacings found in the whole myelin in quantitative terms, thus suggesting the similarity of DIGs and the non-native phases of PMMs induced under the respective conditions.

Materials and methods

Preparation of PMMs

PMMs were prepared from bovine spinal cord according to Haley et al [28] and it was a gift from *Bustos y Beltrán S.A*. abattoir (Córdoba, Argentina) under the supervision of the

veterinary of sanity authority. Briefly, the purification protocol consists of several osmotic shocks and direct as well inverse sucrose gradient centrifugations to discard gray matter constituents according to density. After 3 final rinsing steps in water the myelin membranes were lyophilized and stored at -20 or -70˚C. Chemicals were of analytical degree, purchased from Merck (Germany), and used without further purification.

PMMs retain myelin biochemical composition [29] as well as TEM patterns (S1 and S2 Figs) of isolated myelin [30, 31]. PMMs also show an electron density profile (S3 Fig) close to that of myelin and purified myelin [21].

Isolation of detergent-insoluble glycosphingolipid-rich microdomains (DIGs)

The detergent extraction protocol has been described previously [7]. Briefly, 50 mg of PMMs were hydrated, thawed and extracted with 250 ml of 1% TX-100 in TNE buffer (25 mM Tris-HCl/0.15 M NaCl/5 mM EDTA) at 4˚C for 30 min with occasional mixing. The TX-100 extracts were centrifuged (13,000 g, 4˚C, 10 min) to separate them into detergent-insoluble pellet and detergent-soluble supernatant fractions.

DIGs are enriched in cholesterol, galactocerebroside, cerebroside sulphate, and with low amount of phospholipids. Phosphatidylethanolamine is almost equipartitioned with the soluble supernatant. The major internodal proteins (Folch´s Proteolipid and Myelin Basic Protein) are not found in the DIGs; the paranodal CNPase is also mainly partitioned out of DIGs [7, 8]. S4 Fig in supporting material shows a TEM of DIGs with a pattern different from the one of PMMs.

Small-angle X-ray scattering (SAXS)

SAXS was measured to determine the lamellar periodicity of PMMs and DIGs multilayers under various conditions.

For PMMs sample preparation, 2–3 mg of lyophilized PMMs were introduced in quartz capillaries (Hilgensberg, Malsfeld, Germany) of 1 mm diameter, and 10 μl of aqueous solutions were added. The solutions were: A) pure (bi-distilled) water, B) physiological Ringer´s solution (145 mM NaCl, 6 mM KCl, 2 mM $CaCl_2$, pH 7,4 with 1.5 mM $NaHCO_3/NaH_2PO_4$ buffer), and C) 25 mM $CaCl_2$ in Ringer´s solution. The capillaries were flame sealed and subsequently centrifuged to facilitate the sample hydration. They were then subject to four thawing and cooling cycles (4 to 40˚C) and then stored at 4˚C.

For DIGs sample preparation, lyophilized DIGs were suspended at 25 mg/ml, warmed up to 45˚C to ensure equilibration and filled into the sample holder between two mica plates. A 150 mM NaCl solution was used in replacement to the Ringer's solution and 25 mM $CaCl_2$ was employed to induce compaction. The difference in the solutions used for PMMs and DIGs has negligible effect.

SAXS experiments were carried out at the beamline A2 at Hasylab (DESY, Hamburg, Germany) and at the DO2A:SAXS2 beamline at LNLS (Campinas, Brazil), at fixed wavelength of $\lambda = 1.5$ Å. Scattering signals were recorded either using a linear position-sensitive detector (built by André Gabriel from ILL, EMBL) [32], or a 2D detector (MARCCD 165). In the latter case, radial integration of the Debye-Scherrer rings was performed with the free software Fit2D V12.077 by Andy Hammersley of European Synchrotron Radiation Facility [33]. SAXS intensities are presented as a function of the magnitude of the scattering vector,

$$q = \frac{4\pi}{\lambda}\sin\left(\frac{\theta}{2}\right) \quad (1)$$

where θ is the scattering angle with respect to the incident beam. The corresponding lamellar periodicities d then follow from the Bragg equation as

$$d = 2\pi h/q \tag{2}$$

where $h = 1, 2, \ldots$, is the peak order.

The number n of periodically correlated bilayers under various conditions was obtained by applying the Scherrer equation to the Bragg peak full width at half maximum (w) of a Lorentzian curve:

$$n = \frac{2\pi \times 0.88}{d\sqrt{w^2 - r^2}} \tag{3}$$

where r is the instrumental resolution ($r \approx 0.04$ nm^{-1}).

The diffracting power of native phase was defined [34] by the origin peak of Patterson function:

$$P_{nat} = \sum\nolimits_h \left[\frac{hI_{nat}(h)}{d^2}\right] \tag{4}$$

where $hI_{nat}(h)/d$ is the Lorentz-corrected intensity of the reflection of order h. The integrated $I_{nat}(h)$ was estimated from the areas under the associated Bragg peaks. The fraction of myelin in native phase is expressed as the ratio of the diffracting power P_{native} to the initial amount ($P_{native} + P_{non\text{-}native}$).

The values of SAXS periodicities (d), number of correlated bilayers (n) and Relative Diffracting Power correspond to the mean of two independent determinations.

Neutron diffraction (ND) from solid supported membrane multilayers

The ND measurements were performed at the Institute Laue-Langevin (Grenoble) at the beamline D16, with wavelength $\lambda = 4.54$ Å. Lyophilized PMMs (1 mg) were suspended in 1 ml of bi-distilled water. A 0.5 mL portion of solution/suspension was deposited onto a rectangular (55 x 25 mm^2) Si(100) substrate with native oxide (Si-Mat, Landsberg/Lech, Germany), which was cleaned by a modified RCA method—ultrasonication in acetone, ethanol, and methanol and subsequent immersing in a solution of 1:1:5 (v/v/v) H_2O_2(30%)/NH_4OH(30%)/water at 60˚C for 30 min—[35]. During the process of water evaporation, the amphiphilic molecules self-assemble into planar membrane stacks, aligned parallel with the substrate surface. The PMM-coated wafers were then confined in a sandwich-like liquid cell described elsewhere [36], which brings the multilayers in contact with a thin layer of bulk aqueous medium. The liquid cell, in turn, was inserted into a climate chamber for temperature control. Two different buffers were used: A) 5 mM Hepes + 100 mM NaCl at pH 7.4 and B) the same buffer additionally loaded with 20 mM $CaCl_2$. Buffers were based on D_2O, to enhance the neutron scattering contrast with the hydrogenous PMMs material. Since the membrane multilayers are aligned parallel to the solid support and thus oriented with respect to the incident neutron beam, the measurements involve angular rocking scans, as described earlier for membranes composed of synthetic phospho- and glycolipids [36, 37]. The scattering wave vector component perpendicular to the membrane plane, q_z, assumes the role of q in the SAXS experiments (see previous section) and is given as

$$q_z = \frac{4\pi}{\lambda}\sin(\theta) \tag{5}$$

where θ is the incident angle. The lamellar periodicity is then calculated by replacing q with q_z in Eq 2.

Differential scanning calorimetry (DSC)

A VP-DSC from Microcal, LLC was used with a scan rate of 20˚C/h. Generally, several heating and cooling scans (typically from 4 to 46˚C) were performed to exclude any influence of thermal history. The concentration of PMMs was 20 mg/ml in all the aqueous suspensions: A) bi-distilled water, B) NaCl 100 mM in water and C) $CaCl_2$ 33 mM in water.

Results and discussion

PMMs phase behavior

The phase behavior of PMMs was investigated for various temperatures (4–45˚C) and aqueous solutions. SAXS measurements (see Methods section) were carried out to determine the number of coexisting phases under given conditions, as well as their respective lamellar periodicities d, the amounts of myelin in the native and non-native phases, perpendicular thermal expansivity $\alpha_\perp$ (K^{-1}), and membrane correlation numbers n. Fig 1 shows scattering intensities from PMMs in physiological Ringer's solution as recorded with the 2D-detector, featuring Debye-Scherrer rings corresponding to isotropically-oriented multilamellar samples. The intensity patterns obtained at each temperature are reproducible and independent of the thermal history. The appearance of double-rings at low temperatures is characteristic of the coexistence of two membrane phases with different lamellar periodicities.

Fig 2(A) and 2(B) shows radially integrated SAXS intensities plotted vs. q for PMMs in bi-distilled water (A) and physiological Ringer's solution (B) for various temperatures. At high temperature (> 37˚C), the scattering intensities exhibit only two major peaks, at $q \approx 0.8$ nm^{-1} and $q \approx 1.6$ nm^{-1}, respectively, according to the nomenclature by Kirschner [23] corresponding to the peak orders $h = 2$ and $h = 4$ of a double myelin bilayer with lamellar periodicity of $d \approx 7.9$ nm per bilayer. As the temperature decreases, in both solutions the weak peak of order $h = 1$ becomes increasingly stronger at $q \approx 0.4$ nm^{-1}, which is half the value of the $h = 2$ peak and corresponds to $d \approx 15.8$ nm, the periodicity of the well-known repeating cell unit of native myelin accommodating two 7.9 nm membranes. Further cooling leads to the splitting of the $h = 2$ and $h = 4$ peaks, associated with the emergence of additional peaks, termed h = II and h = IV, corresponding to the formation of an additional phase with larger, "expanded" periodicity. The expanded phase appears to have a repeating unit consisting of a single bilayer according to the fact that no h = I peak is observed. Its periodicity further expands upon cooling, to $8.2 < d < 10$ nm as seen from the shift in the h = II and h = IV peak positions to lower q values. Comparison of Fig 2A and 2B reveals that the phase separation occurs already close to the physiological temperature (25–30˚C) in Ringer's solution, while in water a similar splitting

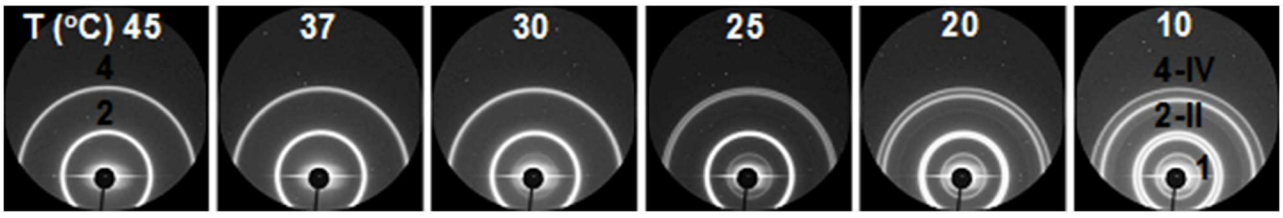

Fig 1. X-ray diffraction pattern of isolated myelin as a function of temperature in Ringer's solution. At high temperature (37–46˚C) two single rings Peaks 2 and 4 are observed. At 30˚C the faint smallest peak (1) is observed near the beamstop. At 25˚C beam splitting is more easily observed in the peak 4 and IV which is also evident in peaks 2 and II at 10˚C.

https://doi.org/10.1371/journal.pone.0184881.g001

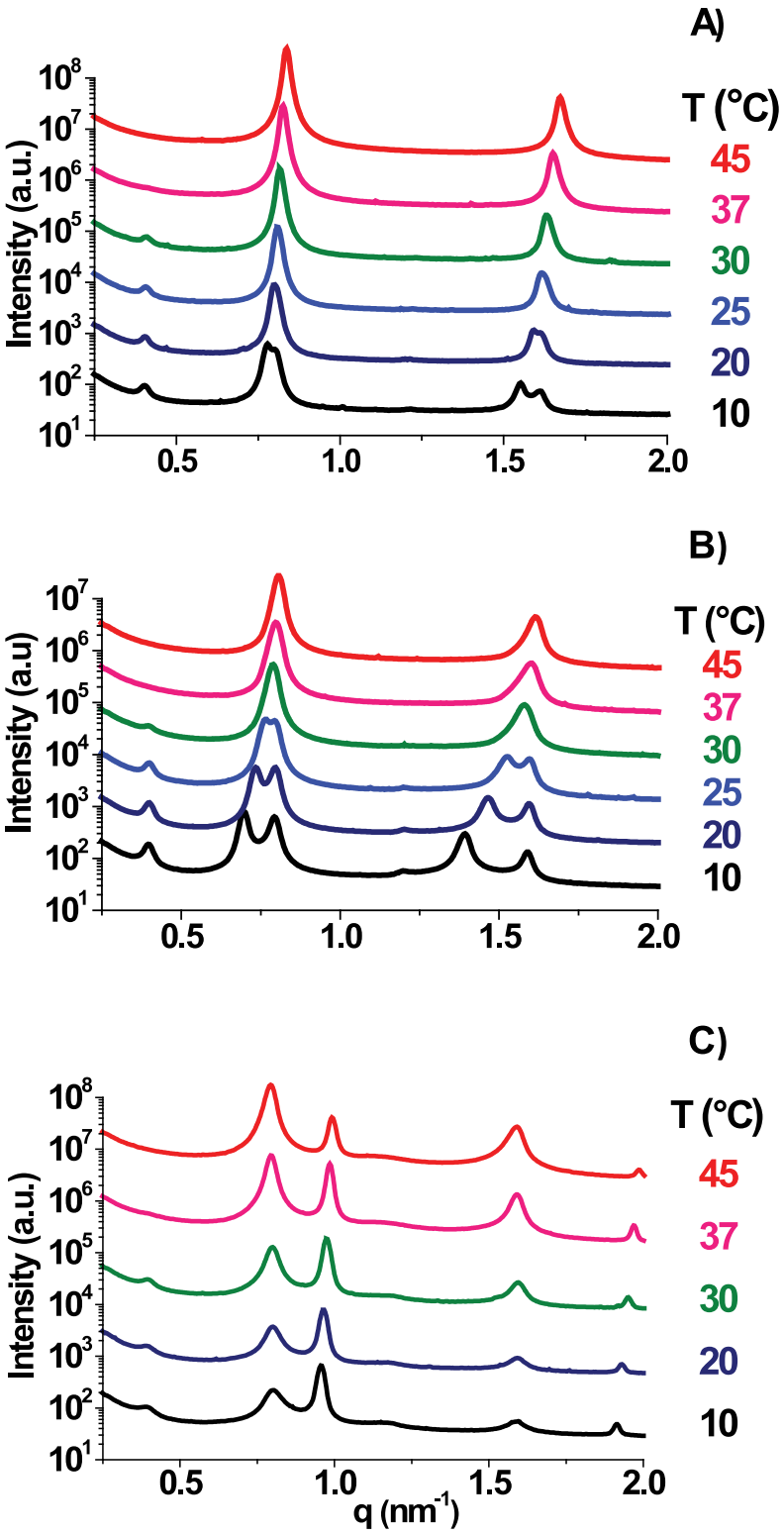

Fig 2. Integrated signals of myelin at different temperatures and in different aqueous conditions. Bi-distilled water (A), Ringer's solution (B) and $CaCl_2$ 25 mM in Ringer's solution (C). In the case of water dominates a simple pattern and only at low temperature the Bragg peaks splits and shifts to lower *q*. The same happens in the case of Ringer's solution but at higher temperature. On the other hand, the response to Ca^{2+} goes in the opposite direction in *q* and it is as a jump (all or nothing) instead of a shift.

https://doi.org/10.1371/journal.pone.0184881.g002

of peaks is observed at 20–25˚C. As shown in Fig 2C, elevated Ca^{2+} concentration leads to splitting of the $h = 2$ and $h = 4$ peaks for all studied temperatures. The h = II and h = IV peaks are, however, shifted to higher q values, corresponding to the emergence of a "compacted", lipid-enriched phase with $5.5 < d < 6.5$ nm, as described in the literature on PMMs and nerve myelin [26, 38]. The native myelin double bilayer of 15.8 nm anyway persists at low T.

The relative fraction of each phase in dependence of the temperature was estimated from the ratio of the diffracting power of each phase to the initial amount [34]. As shown in Fig 3, when starting from low temperatures heating in all studied aqueous solutions induce growth of the native phase at the expense of the non-native phase. Depending on the composition of the aqueous medium, the non-native phase either disappears above a certain temperature (20–25˚C in bi-distilled water, ≈ 25–30˚C in physiological Ringer's solution) or remains partially present in the covered temperature range (at elevated Ca^{2+} concentration).

The thermodynamics of the phase transitions was investigated by DSC. Thermal scans of PMMs are shown in Fig 4. For both bi-distilled water and physiological aqueous solution, the heat capacity C_p exhibits a very broad, endothermic maximum centered at ≈ 26–27˚C, near the phase separation temperature. Upon reaching physiological temperature, where only the native phase remains present, C_p reaches a constant value, indicating the completion of the endothermic transition. This result is consistent with earlier work in similar myelin systems and experimental conditions [39–41]. In contrast, at elevated Ca^{2+} concentration a monotonic increase in C_p with temperature is observed in the entire temperature range, possibly suggesting an ongoing transition. This behavior parallels the variation of C_p when the myelin is heterogeneous in water and physiological conditions and we speculate that this is due to the redistribution of components as inferred from phase amounts (Fig 3). Although the curves

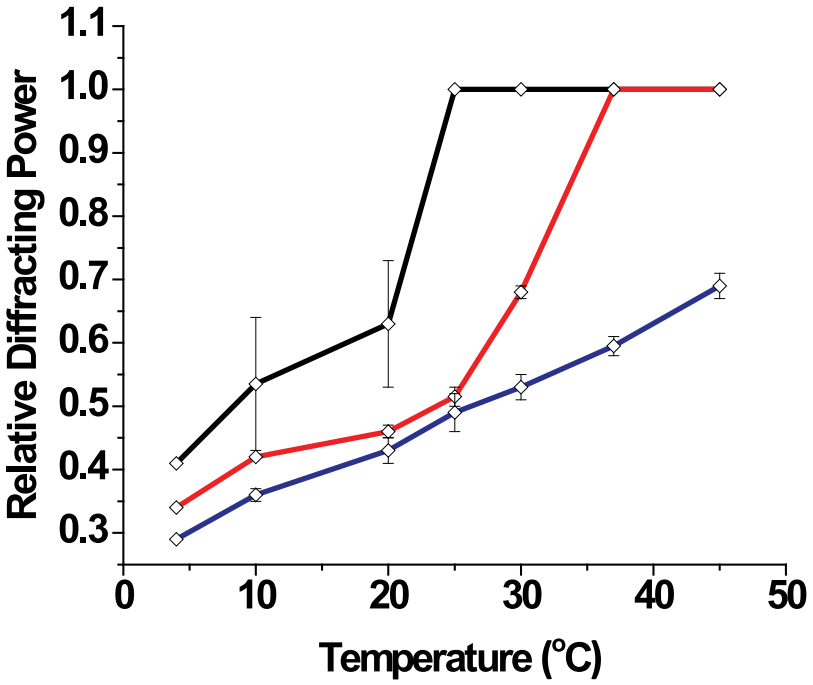

Fig 3. Quantification of the phases as a function of temperature in different conditions. Bi-distilled water (black line), Ringer's solution (red line) and $CaCl_2$ 25 mM in Ringer's solution (blue line). Data is extracted from the ratio of diffracting power of the native phase to the total amount. Clearly, cooling (as in lipid raft isolation protocol) induces a decay of the native phase fraction and a concomitant increment of the non-native phase (not plotted).

https://doi.org/10.1371/journal.pone.0184881.g003

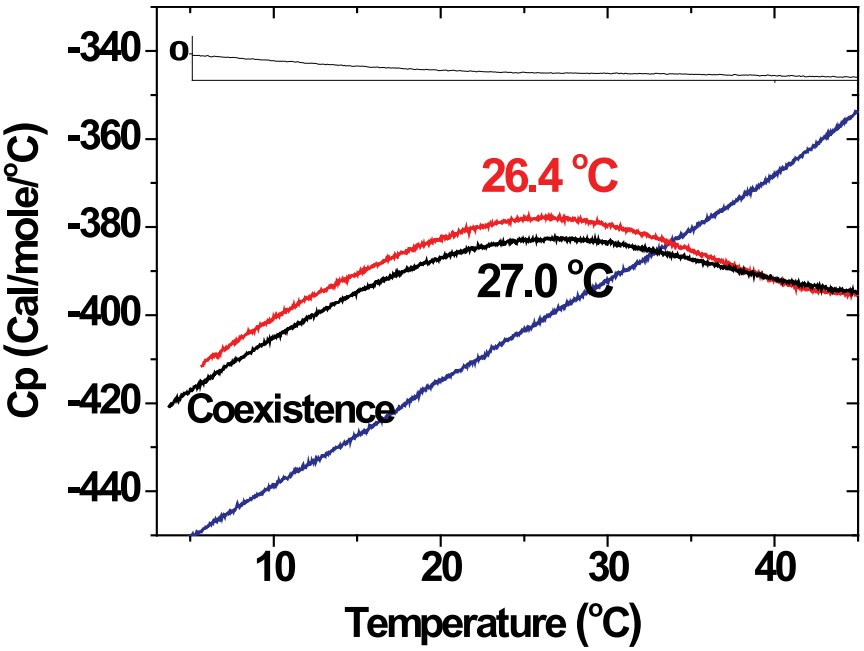

Fig 4. DSC thermograms of myelin (20 Mm) under different aqueous media. In the cases where homogenization takes place–bi-distilled water (black line) and near physiological medium (red line)–a maximum is reached after which a stabilization of the C_p is observed near physiological temperature. In the case of high [Ca^{2+}] (blue line), a continuous variation of C_p according to a phase redistribution of components is observed.

https://doi.org/10.1371/journal.pone.0184881.g004

display only small C_p variations, they are very reproducible. Earlier calorimetry work on PMMs [39, 41] show a broad endothermic peak at 20–30˚C, which has been ascribed to the enthalpies involved in lipid/protein interactions with myelin basic protein (MBP) or Folch´s proteolipid (PLP). In the present work on PMMs we ascribe the broad maxima in C_p to the membrane phase transitions seen by SAXS. These poorly-defined maxima are probably associated with a phase transition of rather low cooperativity. However, the redistribution of components seems to lead to a change in the heat capacity of the system.

To identify protein-rich and lipid-rich phases, the thermal response of the bilayer thickness was analyzed. For the range of temperatures studied, lamellar periodicities d changed linearly with temperature. The perpendicular thermal expansivity ($\alpha_\perp$) of the membrane array was determined from the slopes of the linear functions used to fit the different data, divided by the lamellar periodicities ($\alpha_\perp = [\partial d/\partial T]/d$) [42]. In general, protein-rich domains are thicker and less responsive than lipid-rich domains, which are thinner and more responsive [23, 42, 43]. The q position of the Bragg peaks associated with the Ca^{2+}-induced compacted phase has a response to temperature that is quantitatively accounted for by the well-known negative perpendicular thermal expansivity of lipids undergoing changes in the trans-gauche configuration state, [42, 43] (Table 1). This agrees with the fact that this phase is depleted of intramembrane particles [38]. The same trend is observed in the native phase, but to a lesser extent due to its higher protein fraction [23]. On the other hand, the response of the expanded phase is very strong and cannot be accounted for in terms of perpendicular thermal expansion. Instead, it must be attributed mainly to an increase in the thickness of the interlamellar water layer due to a change in membrane interactions [44].

Periodicity values decay with increments of temperature for all the phases. The expansivities were calculated from the slopes of d versus temperature. The linear fit includes all the

Table 1. Perpendicular thermal expansivity of the different phases in myelin.

Myelin phase	$\alpha_{\perp}$ (K^{-1})
Native	-7.2×10^{-4}
Non-native (expanded)	-5.5×10^{-3}
Non-native (compacted)	-1.3×10^{-3}

https://doi.org/10.1371/journal.pone.0184881.t001

periodicity values from each phase (native, compacted and expanded), regardless of the ionic conditions.

Neutron diffraction on planar geometry array

We have previously reported that Langmuir monolayers derived from PMMs at the air/water interface exhibit phase behavior which is qualitatively like that of spontaneously curved PMMs in aqueous suspensions [26]. To elucidate whether the quantitative differences nonetheless observed are related to the absence of one monolayer or rather to the absence of curvature, we investigate planar, i.e., non-curved, PMMs multilayers on macroscopic solid supports.

As a check of the quality of the orientation on the planar support, the mosaicity for the native phase at 37˚C (Ca^{2+} free) was 0.17˚. After addition of Ca^{2+} the compacted phase had a mosaicity of 0.26˚. Both values show a reasonable orientation for hydrated samples [45].

Fig 5 shows neutron diffraction intensities as a function of q_z for planar PMMs multilayers in physiological buffer at two temperatures, 37˚C and 5˚C. As observed in the SAXS experiments on suspended PMMs (see previous section), the single native phase present at 37˚C upon cooling splits up into two phases, one of which keeps the native periodicity, $d \approx 8.2$ nm, while the other one is expanded to $d \approx 11.0$ nm. The addition of an elevated Ca^{2+} concentration

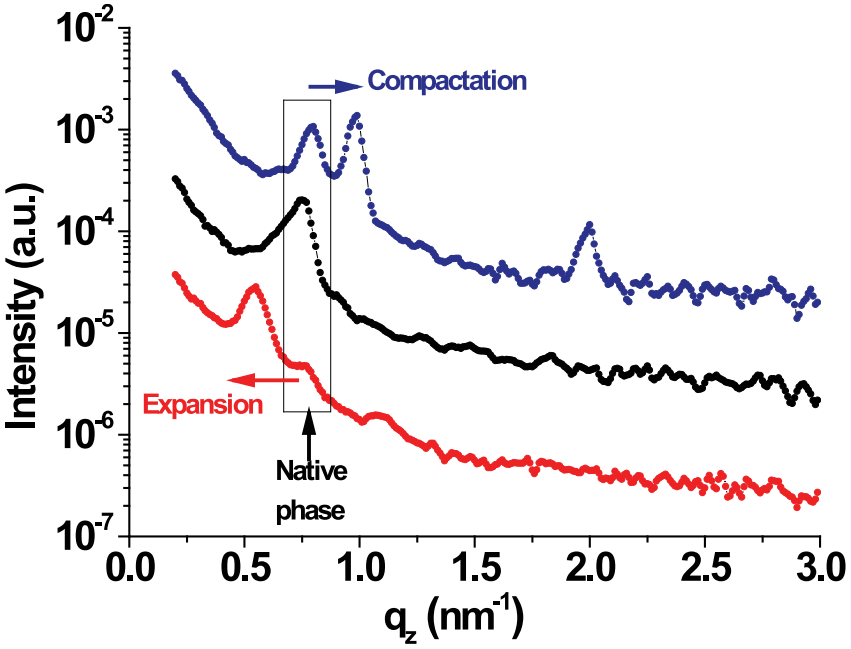

Fig 5. Neutron diffraction signals of multilamellar planar arrays in different media and temperature. The black curve is close to physiological condition. The red curve is the same sample after cooling at 5˚C. Two phases are observed with expansion of the spacing. The blue curve is in the presence of high (Ca^{2+}) at 37˚C; a phase separation takes place in the opposite direction with a compaction.

https://doi.org/10.1371/journal.pone.0184881.g005

Table 2. Neutron diffraction (planar system) periodicities compared to SAXS on equivalent conditions.

	d (nm)—Native phase		*d* (nm)—Compacted phase		*d* (nm)—Expanded phase	
	SAXS	ND	SAXS	ND	SAXS	ND
37˚C–Ca^{2+}-loaded	7,64±0.07	7.9	6.18±0.02	6.4	-	-
37˚C–Ca^{2+}-free	7.6±0.1	8.2	-	-	-	-
4/5˚C–Ca^{2+}-free	7.83±0.07	8.1	-	-	8.9±0.4	11.0

https://doi.org/10.1371/journal.pone.0184881.t002

to the physiological buffer again leads to the emergence of a compacted phase, with $d \approx 6.4$ nm, coexisting with the native phase even at 37˚C in agreement with the SAXS results on suspended PMMs (see Table 2).

Therefore, as a general conclusion; SAXS, ND and Langmuir monolayers [26] measurements agree in qualitative terms, regarding the kind of phase that is generated in particular conditions. The planar geometry appears to allow further separation to the expanded phase in quantitative terms, as compared to the more self-sealed and curved PMMs. Langmuir monolayers cannot be compared in this regard.

Neutron Diffraction data follows the same trend as SAXS data, displaying analogous behavior. The planar systems display periodicities about 0.2 nm longer; except for the expanded phase in which this effect is maximum reaching a difference of 1.6 nm and a more complete transformation of the native myelin in expanded phase (the native Bragg peak is almost residual).

Phase behavior of DIGs

DIGs were investigated by SAXS at isolation conditions (at 4˚C) to compare their periodicity with those of the non-native phases of PMMs. The scattering intensities as a function of *q* are shown in Fig 6. DIGs in physiological ionic strength (5 mM Tris + 150 mM NaCl, Fig 6A), whose periodicity, $d = 9.5$ nm, is close to the $d = 9.4$ nm of the PMMs expanded phase under these conditions. In the presence of elevated Ca^{2+} concentration (Fig 6B) the periodicity of the DIGs fraction is $d = 6.6$ nm, very close to that of the PMMs compacted phase under similar conditions ($d = 6.4$ nm). Thus, we show that the same DIGs fraction can behave as a compacted and as an expanded phase, depending on the ionic milieu conditions.

The similarity of DIGs and the non-native phases of PMMs also manifest in the collective behavior of the membrane multilayers. Namely, as shown in Fig 7, the number *n* of correlated DIGs bilayers, as extracted from the width of the Bragg peaks (see Material and methods), agrees well with the corresponding number for the PMMs non-native phases under the same conditions. For the compacted PMMs phase, $n \approx 14–24$ showing the highest correlation. The expanded PMMs phase, comprising a thick water layer, is poorly correlated ($n \approx 4–6$ irrespective of the temperature). Only for the native phase of PMMs *n* exhibits significant temperature-dependence, changing from $n \approx 5–6$ to $n \approx 15–19$ upon heating from 10˚C to physiological temperature and above. These results agree in general terms with observations of similar myelin systems [14, 21, 38].

There are arguments to think that the presence of detergents modifies the phase diagram of membranes creating or promoting liquid ordered phases [46]. The good point of our approach is that we can detect DIG-like phases in PMMs even in the absence of the detergent. Still there is a possibility that DIGs and non-native phases are not exactly the same [46].

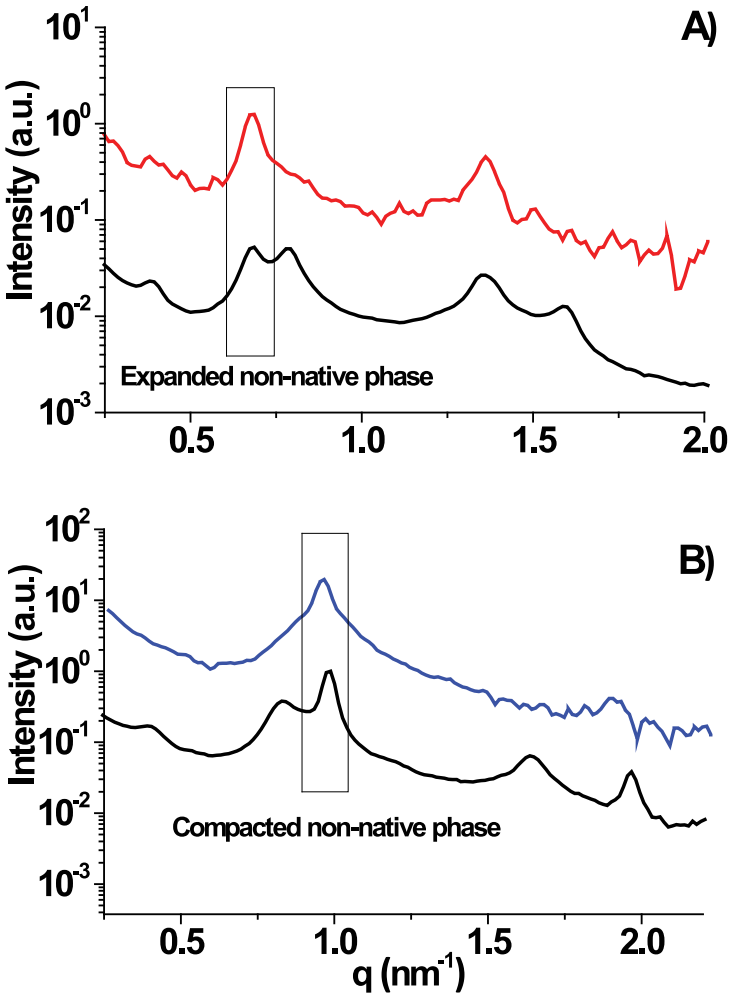

Fig 6. SAXS of DIGs in different ionic conditions at T = 4˚C. In the presence of a physiological buffer (A) the first order peaks for DIGs (red dots) and non-native phase from PMMs (black dots) are respectively at 0.66 and 0.67 nm^{-1} indicating lamellar spacings of 9.5 nm and 9.4 (expanded phase). In the presence of $CaCl_2$ 25 mM (B) the first order peaks for DIGs (blue dots) and non-native phase from PMMs (black dots) are respectively at 0.96 and 0.98 nm^{-1} indicating lamellar spacings of 6.6 and 6.4 nm (compacted phase).

https://doi.org/10.1371/journal.pone.0184881.g006

Conclusion

Classical work pictured nerve myelin as a uniform membrane, phase separation only being obtained after relatively harsh treatments involving osmotic shocks or dehydration [23, 27]. While the expanded and compacted non-native phases of nerve myelin have been identified long ago [38], they were not discussed in the context of putative myelin lipid rafts.

Our group previously demonstrated phase coexistence also in Langmuir monolayers of lipid/protein mixtures derived from PMMs [47, 48]. Nevertheless, the monolayers can also get homogeneous according to lateral packing and ionic media [26] and unexplored variables (temperature, for instance). Therefore, explorations in other systems are mandatory in order to approach new experimental situations. In this sense, PMMs tend to mimic the behavior of nerve myelin in general terms regarding TEM appearance, native spacing, electron density profile and expansion-contraction in response to environmental conditions. [21, 26, 49].

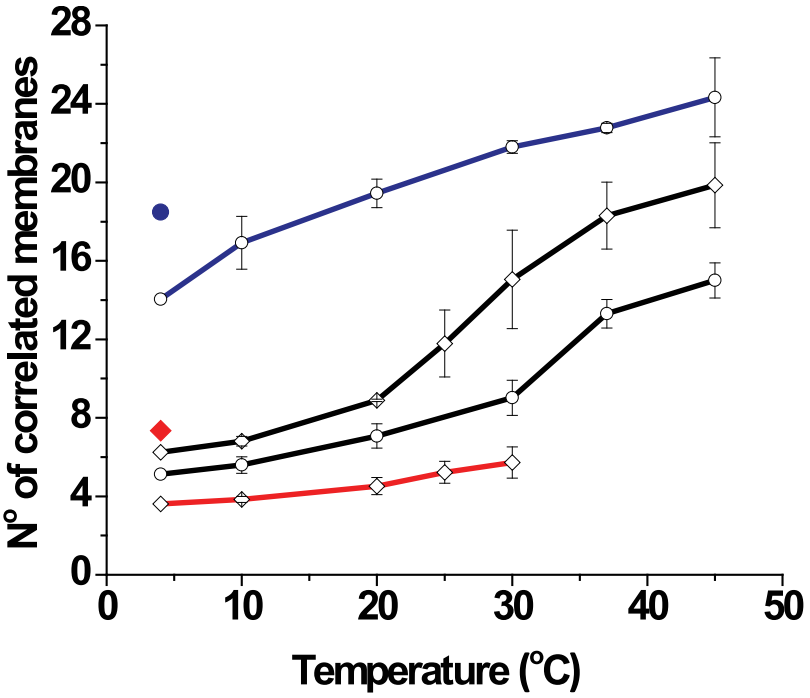

Fig 7. Number (*n*) of correlated membranes for the different phases as a function of temperature for whole myelin (empty) and DIGs (filled). In black is marked the *n* for the native period, in red for the expanded period and in blue for the compact period. In the presence of physiological (diamonds) and high [Ca^{2+}] (circles) media.

https://doi.org/10.1371/journal.pone.0184881.g007

In this work, we clearly show that the cooling of PMMs by about 10–20˚C below 37˚C induces the phase separation, in a way that is not collectively detectable in nerve myelin. Nevertheless, precursors of phase separation are observed by EM as regions of detachment between the membranes at the extracellular space upon cooling (arrows of Fig 7 in [14]). The presence of phase transitions in nerve membranes at about 25˚C was discussed to be related to electromechanical pulse propagation in nerves [50].

The striking similarities in terms of structure and collective behavior of the DIGs and the non-native phases of PMMs at the extraction temperature strongly indicate that the two membranes have very similar constitution. Conversely, this notion implies that the expanded and compacted non-native phases of PMMs are virtually identical [51] and basically differ only with respect to their transverse (interlamellar) interactions under different conditions (see Fig 6). In view of the significant temperature-dependence of fractional weight and, thus, composition of native and non-native PMMs phases, their similarity to DIGs further indicates that the composition of the isolated DIGs significantly depends on the extraction temperature and must therefore be expected to deviate from that of putative rafts transiently forming in myelin at physiological temperature.

Our own studies in Langmuir monolayers strongly support this view [26] of a simple lateral phase separation but with different transverse interlamellar interactions according to the ionic media. Further work in this direction is currently carried out.

The phases shown here are detectable under non-physiological conditions, and one of those conditions (low T) is employed to isolate DIGs, that represent lipid rafts *in vivo* according to some authors. We identify the DIGs as the PMMs non-native phase induced by cooling. Low T is employed during DIGs or raft isolation, not to avoid growth of microorganisms or

degradation of the membrane. Rather, cooling alters the membranes and stabilizes DIGs. If DIGs isolation protocol is performed at 37˚C, almost no rafts or DIGs are obtained. Low T is used in order to operationally obtain DIGs, but our own results put in question (although not discard) its existence and/or identity at physiological temperature.

Supporting information

S1 Fig. Full field TEM of PMMs at low magnification (60.000x). Pellets of PMMs and DIGs were fixed overnight in 2.5% glutaraldehyde buffered with 0.5 M cacodylate, rinsed three times in distilled water and postfixed in 1% osmium tetroxide buffered with 0.5 M cacodylate at pH = 7. After rinsing, samples were stained in 0.5% uranyl acetate overnight, dehydrated through a graded series of acetone and embedded in epoxy resin. Finally, the thin sections were stained with lead citrate at pH = 12 for 15 minutes. Samples were examined in a JEOL 1220 EXII electron microscope. The micrograph shows a typical pattern of isolated myelin (Kartigashan and Kirschner, 1988; Larocca and Norton 2006). The sample was reconstituted by rehydration of lyophilized PMMs of bovine spinal cord myelin. The characteristic stack of membranes is clearly seen in the image, as well as the rounded shape of some of the stacks.
(TIF)

S2 Fig. TEM of PMMs viewed at high magnification (300.000x). The alternation of major dense and intraperiod lines is observed. The major dense lines period is around 13 nm, a little shrink from the normal period as usual, due to artefacts of preparation (Hollingshead and Kirschner 1979).
(TIF)

S3 Fig. Electron density profile of PMMs in water at 25˚C. The sample was reconstituted from lyophilized myelin powder. The characteristic pattern of myelin consisting in two asymmetric bilayers is observed. Phases are shown in the inset.
(EPS)

S4 Fig. TEM of DIGs viewed at high magnification (400.000x). The aspect of the membranes does not match the original one of S1 and S2 Figs.
(TIF)

S1 File. Primary data.
(RAR)

Acknowledgments

We thank HASYLAB-Deutsches Elektronen Synchrotron (DESY), Hamburg, Germany (beamline A2 at DORIS), Laboratório Nacional de Luz Síncrotron, Campinas, Brazil (beamline SAXS2) and Beamline D16 at the Institute Laue Langevin (Grenoble) for measurement times.

Author Contributions

Conceptualization: Julio M. Pusterla, Rafael G. Oliveira.

Data curation: Julio M. Pusterla, Emanuel Schneck, Sérgio S. Funari, Bruno Démé, Rafael G. Oliveira.

Formal analysis: Julio M. Pusterla, Emanuel Schneck, Sérgio S. Funari, Bruno Démé, Rafael G. Oliveira.

Funding acquisition: Rafael G. Oliveira.

Investigation: Julio M. Pusterla, Motomu Tanaka, Rafael G. Oliveira.

Methodology: Julio M. Pusterla, Emanuel Schneck, Sérgio S. Funari, Bruno Démé, Motomu Tanaka, Rafael G. Oliveira.

Project administration: Rafael G. Oliveira.

Software: Emanuel Schneck, Bruno Démé.

Writing – original draft: Julio M. Pusterla, Emanuel Schneck, Bruno Démé, Motomu Tanaka, Rafael G. Oliveira.

Writing – review & editing: Julio M. Pusterla, Emanuel Schneck, Rafael G. Oliveira.

References

1. Taylor CM, Marta CB, Bansal R, Pfeiffer S. The Transport, Assembly and Function of Myelin Lipids. In: Lazzarini RA, Griffin JW, Lassmann H, Nave K, Miller R, Trapp BD, editors. Myelin Biology and Disorders. 1: Elsevier Academic Press; 2004.
2. Keller SL, Pitcher WH 3rd, Huestis WH, McConnell HM. Red Blood Cell Lipids Form Immiscible Liquids. Physical review letters. 1998; 81(22):5019–22.
3. Veatch SL, Cicuta P, Sengupta P, Honerkamp-Smith A, Holowka D, Baird B. Critical fluctuations in plasma membrane vesicles. ACS chemical biology. 2008 May 16; 3(5):287–93. https://doi.org/10.1021/cb800012x PMID: 18484709.
4. Jin AJ, Edidin M, Nossal R, Gershfeld NL. A singular state of membrane lipids at cell growth temperatures. Biochemistry. 1999 Oct 5; 38(40):13275–8. PMID: 10529201.
5. Rosetti CM, Oliveira RG, Maggio B. The Folch-Lees proteolipid induces phase coexistence and transverse reorganization of lateral domains in myelin monolayers. Biochimica et biophysica acta. 2005 Feb 01; 1668(1):75–86. https://doi.org/10.1016/j.bbamem.2004.11.009 PMID: 15670733.
6. Min Y, Alig TF, Lee DW, Boggs JM, Israelachvili JN, Zasadzinski JA. Critical and off-critical miscibility transitions in model extracellular and cytoplasmic myelin lipid monolayers. Biophysical journal. 2011 Mar 16; 100(6):1490–8. https://doi.org/10.1016/j.bpj.2011.02.009 PMID: 21402031.
7. Kim T, Pfeiffer SE. Myelin glycosphingolipid/cholesterol-enriched microdomains selectively sequester the non-compact myelin proteins CNP and MOG. Journal of neurocytology. 1999 Apr-May; 28(4–5):281–93. PMID: 10739571.
8. Arvanitis DN, Yang W, Boggs JM. Myelin proteolipid protein, basic protein, the small isoform of myelin-associated glycoprotein, and p42MAPK are associated in the Triton X-100 extract of central nervous system myelin. Journal of neuroscience research. 2002 Oct 01; 70(1):8–23. https://doi.org/10.1002/jnr.10383 PMID: 12237860.
9. Taylor CM, Coetzee T, Pfeiffer SE. Detergent-insoluble glycosphingolipid/cholesterol microdomains of the myelin membrane. Journal of neurochemistry. 2002 Jun; 81(5):993–1004. PMID: 12065611.
10. Schmitt FO, Bear RS, Clark GL. X-ray diffraction studies on nerve. Radiology. 1935; 25:131–51.
11. Inouye H, Kirschner D. Myelin: A one-dimensional biological "crystal" for x-ray and neutron scattering. In: Sedzik J, Riccio P, editors. Molecules: Nucleation, aggregation and crystallization: Beyond medical and other implications World Scientific Publishing Co.; 2009. p. 73–5.
12. Kirschner DA, Hollingshead CJ, Thaxton C, Caspar DL, Goodenough DA. Structural states of myelin observed by x-ray diffraction and freeze-fracture electron microscopy. The Journal of cell biology. 1979 Jul; 82(1):140–9. PMID: 479295.
13. Kirschner DA, Hollingshead CJ. Processing for electron microscopy alters membrane structure and packing in myelin. Journal of ultrastructure research. 1980 Nov; 73(2):211–32. PMID: 6163867.
14. Mateu L, Luzzati V, Vonasek E, Mateu E, Villegas GM, Vargas R. Order-disorder phenomena in myelinated nerve sheaths: V. Effects of temperature on rat sciatic and optic nerves, and structural differences between the two types of nerve. Journal of molecular biology. 1995 Jan 13; 245(2):110–25. PMID: 7799430.
15. Luzzati V, Mateu L, Marquez G, Borgo M. Structural and electrophysiological effects of local anesthetics and of low temperature on myelinated nerves: implication of the lipid chains in nerve excitability. Journal of molecular biology. 1999 Mar 12; 286(5):1389–402. https://doi.org/10.1006/jmbi.1998.2587 PMID: 10064705.

16. Elkes J, Finean JB. Effects of solvents on the structure of myelin in the sciatic nerve of the frog. Experimental cell research. 1953; 4(1):82–95.
17. Worthington CR, Worthington AR. Effect of heat on frog sciatic nerve determined by X-ray diffraction. Internacional Journal of Biological Macromolecules. 1981; 3(3):159–64.
18. Finean JB, Hutchinson AL. X-ray diffraction studies of lipid phase transitions in cholesterol-rich membranes at sub-zero temperatures. Chemistry and physics of lipids. 1988 Jan; 46(1):63–71. PMID: 3338100.
19. Chia LS, Thompson JE, Moscarello MA. Alteration of lipid-phase behavior in multiple sclerosis myelin revealed by wide-angle x-ray diffraction. Proceedings of the National Academy of Sciences of the United States of America. 1984 Mar; 81(6):1871–4. PMID: 6584921.
20. Sedzik J, Toews AD, Blaurock AE, Morell P. Resistance to disruption of multilamellar fragments of central nervous system myelin. Journal of neurochemistry. 1984 Nov; 43(5):1415–20. PMID: 6491660.
21. Inouye H, Karthigasan J, Kirschner DA. Membrane structure in isolated and intact myelins. Biophysical journal. 1989 Jul; 56(1):129–37. https://doi.org/10.1016/S0006-3495(89)82658-X PMID: 2752082.
22. Sedzik J, Blaurock AE. Myelin vesicles: what we know and what we do not know. Journal of neuroscience research. 1995 Jun 1; 41(2):145–52. https://doi.org/10.1002/jnr.490410202 PMID: 7650750.
23. Kirschner D, Ganser AL, Caspar DL. Diffraction Studies of Molecular Organization and Membrane Interactions in Myelin. In: Morell P, editor. Myelin. Second Edition ed. New York: Plenum Press; 1984. p. 51–91.
24. Denninger AR, Deme B, Cristiglio V, LeDuc G, Feller WB, Kirschner DA. Neutron scattering from myelin revisited: bilayer asymmetry and water-exchange kinetics. Acta crystallographica Section D, Biological crystallography. 2014 Dec 01; 70(Pt 12):3198–211. https://doi.org/10.1107/S1399004714023815 PMID: 25478838.
25. Denninger AR, Breglio A, Maheras KJ, LeDuc G, Cristiglio V, Deme B, et al. Claudin-11 Tight Junctions in Myelin Are a Barrier to Diffusion and Lack Strong Adhesive Properties. Biophysical journal. 2015 Oct 06; 109(7):1387–97. https://doi.org/10.1016/j.bpj.2015.08.012 PMID: 26445439.
26. Oliveira RG, Schneck E, Funari SS, Tanaka M, Maggio B. Equivalent aqueous phase modulation of domain segregation in myelin monolayers and bilayer vesicles. Biophysical journal. 2010 Sep 8; 99 (5):1500–9. https://doi.org/10.1016/j.bpj.2010.06.053 PMID: 20816062.
27. Worthington CR, McIntosh TJ. An x-ray study of the condensed and separated states of sciatic nerve myelin. Biochimica et biophysica acta. 1976 Jul 1; 436(3):707–18. PMID: 952915.
28. Haley JE, Samuels FG, Ledeen RW. Study of myelin purity in relation to axonal contaminants. Cellular and molecular neurobiology. 1981 Jun; 1(2):175–87. PMID: 6179624.
29. Oliveira RG, Calderon RO, Maggio B. Surface behavior of myelin monolayers. Biochimica et biophysica acta. 1998 Mar 06; 1370(1):127–37. PMID: 9518579.
30. Larocca JN, Norton WT. Subcellular Fractionation and Isolation of Organelles. Current Protocols in Cell Biology. 33: John Wiley & Sons, Inc.; 2006.
31. Karthigasan J, Kirschner DA. Membrane interactions are altered in myelin isolated from central and peripheral nervous system tissues. Journal of neurochemistry. 1988 Jul; 51(1):228–36. PMID: 3132532.
32. Petrascu AM, Koch M. A beginners' guide to gas-filled proportional detectors with delay line readout. J Macromol Sci Phys B. 1998; 37(4):463–83.
33. Hammersley A, Svensson SO, Hanfland M, Fitch AN, Hausermann D. Two-dimensional detector software: from real detector to idealised image or two-theta scan. High Pressure Research: An International Journal. 1996; 14:235–48.
34. Kirschner DA, Caspar DL. Myelin structure transformed by dimethylsulfoxide. Proceedings of the National Academy of Sciences of the United States of America. 1975 Sep; 72(9):3513–7. PMID: 1059139.
35. Kern W, Puotinen D. Cleaning Solutions Based on Hydrogen Peroxide for Use in Silicon Semiconductor Technology. RCA review; a technical journal 1970; 31:187–206.
36. Schneck E, Rehfeldt F, Oliveira RG, Gege C, Deme B, Tanaka M. Modulation of intermembrane interaction and bending rigidity of biomembrane models via carbohydrates investigated by specular and off-specular neutron scattering. Physical review E, Statistical, nonlinear, and soft matter physics. 2008 Dec; 78(6 Pt 1):061924. https://doi.org/10.1103/PhysRevE.78.061924 PMID: 19256885.
37. Schneck E, Deme B, Gege C, Tanaka M. Membrane adhesion via homophilic saccharide-saccharide interactions investigated by neutron scattering. Biophysical journal. 2011 May 04; 100(9):2151–9. https://doi.org/10.1016/j.bpj.2011.03.011 PMID: 21539782.

38. Melchior V, Hollingshead CJ, Caspar DL. Divalent cations cooperatively stabilize close membrane contacts in myelin. Biochimica et biophysica acta. 1979 Jun 13; 554(1):204–26. PMID: 454600.

39. Moscarello MA, Neumann AW, Wood DD. Thermotropic phase transitions in normal human myelin as observed in a sensitive microcalorimeter. Biochimica et biophysica acta. 1983; 728:201–5.

40. Johnston DS, Chapman D. A calorimetric study of the thermotropic behaviour of mixtures of brain cerebrosides with other brain lipids. Biochimica et biophysica acta. 1988 Apr 22; 939(3):603–14. PMID: 3355836.

41. Ruiz-Sanz J, Ruiz-Cabello J, Lopez-Mayorga O, Cortijo M, Mateo PL. Thermal stability of bovine-brain myelin membrane. European biophysics journal: EBJ. 1992; 21(3):169–78. PMID: 1425472.

42. Pan J, Heberle FA, Tristram-Nagle S, Szymanski M, Koepfinger M, Katsaras J, et al. Molecular structures of fluid phase phosphatidylglycerol bilayers as determined by small angle neutron and X-ray scattering. Biochimica et biophysica acta. 2012 Sep; 1818(9):2135–48. https://doi.org/10.1016/j.bbamem.2012.05.007 PMID: 22583835.

43. Sackmann E. Physical Basis of Self-Organization and Function of Membranes: Physics of Vesicles. In: Lipowsky R, Sackmann E, editors. Structure and Dynamics of Membranes—From Cells to Vesicles. Handbook of Biological Physics. 1A. Amsterdam: North-Holland; 1995. p. 213–305.

44. Schlaich A, Kowalik B, Kanduc M, Schneck E, Netz RR. Physical mechanisms of the interaction between lipid membranes in the aqueous environment. Physica A: Statistical Mechanics and its Applications. 2015; 418:105–25.

45. Nagle JF, Akabori K, Treece BW, Tristram-Nagle S. Determination of mosaicity in oriented stacks of lipid bilayers. Soft matter. 2016 Feb 14; 12(6):1884–91. https://doi.org/10.1039/c5sm02336j PMID: 26677063.

46. Heerklotz H. Triton promotes domain formation in lipid raft mixtures. Biophysical journal. 2002 Nov; 83(5):2693–701. https://doi.org/10.1016/S0006-3495(02)75278-8 PMID: 12414701.

47. Oliveira RG, Maggio B. Epifluorescence microscopy of surface domain microheterogeneity in myelin monolayers at the air-water interface. Neurochemical research. 2000 Jan; 25(1):77–86. PMID: 10685607.

48. Oliveira RG, Maggio B. Compositional domain immiscibility in whole myelin monolayers at the air-water interface and Langmuir-Blodgett films. Biochimica et biophysica acta. 2002 Apr 12; 1561(2):238–50. PMID: 11997124.

49. Inouye H, Kirschner DA. Membrane interactions in nerve myelin. I. Determination of surface charge from effects of pH and ionic strength on period. Biophysical journal. 1988 Feb; 53(2):235–45. https://doi.org/10.1016/S0006-3495(88)83085-6 PMID: 3345332.

50. Heimburg T, Jackson AD. On soliton propagation in biomembranes and nerves. Proceedings of the National Academy of Sciences of the United States of America. 2005 Jul 12; 102(28):9790–5. https://doi.org/10.1073/pnas.0503823102 PMID: 15994235.

51. Worthington CR, McIntosh TJ, Lalitha S. An x-ray study of the effect of enzymes on frog sciatic nerve myelin. Archives of biochemistry and biophysics. 1980 May; 201(2):429–36. PMID: 7396515.